

---

# Development of a small-scale actuator disk

---

*Author*

SANNE DE JONG HELVIG

*Supervisor*

JASON HEARST

December 4, 2019



**NTNU – Trondheim**  
Norwegian University of  
Science and Technology

# Table of Contents

<b>1</b>	<b>Introduction</b>	<b>2</b>
1.1	Problem formulation . . . . .	2
<b>2</b>	<b>Background</b>	<b>3</b>
2.0.1	Experimentally . . . . .	6
2.0.2	Use in CFD simulations . . . . .	7
2.0.3	Developing the actuator disk . . . . .	8
<b>3</b>	<b>Method</b>	<b>10</b>
3.1	Experimental setup . . . . .	10
3.1.1	Force measurer, wind tunnel and associated equipment . . . . .	10
3.1.2	The rig . . . . .	11
3.2	Wind turbine models . . . . .	11
3.3	The actuator disks . . . . .	11
3.3.1	Computer-aided design and 3D printing . . . . .	11
3.3.2	Design of the tower . . . . .	12
3.3.3	Actuator disk design . . . . .	12
3.4	Testing . . . . .	13
3.5	Calculations . . . . .	14
<b>4</b>	<b>Results &amp; Discussion</b>	<b>15</b>
4.1	Rotational WT model . . . . .	15
4.2	Drag on the ADs . . . . .	17
4.3	Noise . . . . .	18
4.4	Possible sources of error . . . . .	18
<b>5</b>	<b>Future work</b>	<b>21</b>
<b>6</b>	<b>Conclusion</b>	<b>22</b>

# Figures

4.1	The drag coefficient for the rotating WT models, obtained through four rounds of measurements. . . . .	16
4.2	The measured drag for the rotating WT models, obtained through four rounds of measurements. . . . .	17
4.3	The average drag coefficient for the rotational WT models for each wind velocity, based on the four conducted measurements, after removing the assumed wrongful outliers. . . . .	18
4.4	Using the solid disk. . . . .	18
4.5	Using the disks with 60% solidity. . . . .	19
4.6	The drag coefficient for the disks with 60% solidity. . . . .	19
4.7	The drag coefficient for the disks with 40% and 35% solidity, compared to the average drag coefficient of the rotating disks. . . . .	20

# Abstract

# Chapter 1

## Introduction

In a world with a growing population, growing standards of living, and with it, a growing need for energy, simultaneous with an increasing focus on sustainability and environmentally friendly solutions, renewable energy has never been more relevant. The amount of onshore and offshore wind power is increasing, and numerous companies are working to find their role in the new market. Finding efficient solutions within wind power is an important aim, and researchers are using both simulations and experimental methods in order to explore different possibilities.

However, in both methods, modeling a wind farm with moving blades is often extremely complicated. Thus, simplifications, such as the actuator disk, are commonly adopted. The idea of the actuator disk is that it produces the same drag as the wind turbine, resulting in similar bulk characteristics in the wake. The physical wind tunnel analogue to an actuator disk is a static, porous disk. However, at this point in time, there are no clear directions and no scientific consensus on how to design and make these porous disks in order to mimic rotating turbines.

### 1.1 Problem formulation

The objective of the project described in this thesis is to develop a static, porous disk that has approximately matched characteristics to a small rotating wind turbine model provided by KTH, by matching the produced drag. In order to achieve this, the drag of the spinning wind turbine models are measured, and a variety of small-scale actuator disks are designed and 3D printed before drag measurements of the disks are conducted. Based on the results, the design will be honed in order to match the drag as closely as possible.

# Chapter 2

## Background

Within the field of wind turbine aerodynamics, the actuator disk theory describes the simplest way to model a rotating turbine. The actuator disk is a non-rotating disk, physically modeled as a static porous disk. The idea is that the actuator disk produces the same drag as a moving turbine, resulting in the same bulk characteristics in the wake.

The drag on the wind turbine models is the force in the direction parallel to the direction of the wind. The drag coefficient is further defined as

$$C_d = \frac{D}{\frac{1}{2} * \rho * u^2 * A} \quad (2.1)$$

where  $\rho$  is density,  $u$  is the flow velocity and  $A$  is the reference area.

The drag on an object changes as the velocity changes. According to theory,  $C_d$  increases as  $Re$  increases and then  $C_d$  levels off at  $Re \simeq 10^3$ , after which it remains approximately constant within the boundary of laminar flow. So this is the typical profile to expect when conducting drag measurements with varying  $Re$ . Here, Reynolds number is defined as

$$Re = \frac{\rho * u * L}{\mu} \quad (2.2)$$

where  $\rho$  is density,  $u$  is velocity,  $L$  is characteristic length and  $\mu$  is the dynamic viscosity. For Reynolds number lower than  $\simeq 5 * 10^5$  the flow is laminar, which is the type of flow relevant for this project.

The porosity is a measure of the permeable area of the disc and is defined as the ratio between the open area and the total area of the disc.

The renewed interest in wind energy originated in part from large funding programs by the American and European governments and from the realization that wind energy will be

---

a important contributor to production of affordable and clean energy in the next decades. A contribution to the overall electricity production of up to 20% is aimed by 2030, but to realize these targets, larger wind farms covering increasingly larger surface areas are required [12]. They wind turbines will grow not only in size, but also in capacity and money invested [3].

Current utility-scale turbines extend a significant distance into the atmospheric boundary layer, which is naturally turbulent [14] [11]. Further, placing the turbines in wind farms is the most economic and efficient when it comes to planning, use of land and infrastructure, and maintenance [14]. Thus, wind turbines are permanently exposed to turbulence, either within the wind or when downstream turbines are hit by the turbulent wake created by upstream rows of turbines and their rotating turbine blades [14] [11].

Within a wind farm, as kinetic energy has been extracted from the wind and converted into electricity, the wind speeds do not recover to their freestream value after encountering the first row of turbines, and thus the wind speeds hitting subsequent turbines are lower than the freestream value [3]. Thus, the wake from the upstream wind turbines determine how much power a downstream turbine can generate and which mechanical loads it experiences, meaning that the study and characterization of wind turbine wakes has become an important research area. [14] [11] When turbine spacing and wind farm layouts are considered in a conventional approach, decisions are made based on the desire to limit the wake-induced fatigue loads on downstream turbines [12].

Variability in power output from wind turbines due to unsteady characteristics of the ABL is a challenge for the integration of large amounts of wind energy into the electricity grid, and the need for fill-in power and stronger components made to withstand unsteady loading turns the problem into that of a cost-minimizing problem, in order for wind energy to achieve the desired market share [5]

Studies of the interaction of large wind farms and the ABL, and how the wake develops and interacts with downstream WT arrays, are currently not prevalent, and improved knowledge and understanding of the interaction is necessary [12] [5] [16] [11] [1]. With improved understanding of this type of flows, wind farm developers can plan better-performing, less maintenance-intensive and longer-lasting wind farms, and manufacturers could create better fatigue load-mitigating designs [11].

Field tests are being carried out, but such approaches are expensive, difficult and by their nature incapable of being completely controlled [16]. Wind tunnel measurements have the advantage over full-scale experiments that the inflow and boundary conditions can be carefully controlled, and thus they can bring additional insight. [5]. Additionally, a wide range of inflow conditions can be tested and the created wake can be studied [16]. However, it should be mentioned that there is a need for increased amounts of data from actual wind farms, to evaluate whether experimental results are representative for the actual case.

A challenge for studying wind farms in wind tunnels is performing measurements with sufficiently high temporal and spatial resolution for a turbine array containing a large number of model turbines [5]. Therefore, small-scale turbines are relevant for experiments, and allow for extensive flow mapping studies to be conducted without the requirement of con-

---

structing scale turbines or the cost associated with large experimental test facilities[7]. The experts workshop organized by ForWind-Uni Oldenburg in 2018 on Wind Energy Science & Wind Tunnel Experiments agreed to qualify the smallest wind turbine models, with a rotor diameter less than 0.5 m, as wake-generating turbine models, independent on whether they are steady or rotating models [1].

However, using rotating blades for such small rotors, and building and operating 100 of them in a wind tunnel is not practical, but rather complex and costly. In addition, scaled rotating wind turbine models have inherent limitations since perfect flow similarity is not possible due to large scale differences. [5]. Rotating wind turbines can be compared to porous media due to their significant amount of flow-through. The question remains whether and to what extend it is possible to use simplified, non-rotating turbine models [14].

In order to study the wake, several numerical and physical modeling approaches are used. Some model the wind turbine with the simplest model, the AD concept, adding a drag source within the surface swept by the blades [2]. Porous disks are momentum sinks that does not directly extract energy from the flow, but instead dissipated kinetic energy of the incoming wind by generating small-scale turbulence in the near wake of the disk [10]. The simple but efficient actuator disk may be used as a simple method for simulating horizontal axis turbines.

Multiple experimental studies concerning ADs have already been conducted. Some are at the stage of developing the AD itself.

For example, Pierella and Sætran (2010) [15] studied the flow behind two circular grids of equal diameter and porosity but different mesh geometry. They used a biplane mesh, which turned out to produce a non-axisymmetric wake, and a monoplane mesh, giving an axisymmetric wake. The two wakes had different characteristics and the disks had different drags.

Earlier this year, nine research teams organized a round-robin measurement campaign of the wake of two porous discs in a homogeneous and low turbulent flow, performing similar wake measurements in different wind tunnels. [1] In general, results collapsed reasonably well across facilities.

Researchers such as Cannon et al. (1993) [6] have studied the wakes behind porous disks of varying solidity.

Others have gone further, and are moving towards the stage of using the actuator disks as simplifications for wind turbine models.

Bossuyt et al (2016) [5] used 100 porous disk models to model a wind farm in a wind tunnel at different layouts, in order to study power output variability and unsteady loading in a turbulent boundary layer.

Also [13] did analysis on the flow field around horizontal axis tidal turbines using mesh disks as rotor simulators.

In 1981, Sforza et al [16] used porous disks to simulate the effect of a wind turbine in



---

order to investigate the wake, using both experimental and numerical methods.

[14] investigated and compared an actuator disc and a model wind turbine exposed to different uniform turbulent inflows, investigating the most variables. In the far wake, the wakes of both are similar. The results are independent on the inflow conditions. Velocity and turbulence intensity was different in the near wake.

A first requirement for a scaled wind turbine representation is a correct characterization of the wake structure (Theunissen et al 2015). When creating an AD to represent a WT, the starting point is often to match the diameter and the drag.

Studies conducted so far has a general agreement on the following terms. The near wake differs between the two models, as the turbulence in terms of the AD is produced by a grid, while rotating turbines introduce rotational momentum, tip and hub vortices and turbulence from the blades (Zhang 2012). The difference in flow behaviour close to the model, especially prominent in terms of velocity deficit and turbulence intensity, is thus caused by fundamentally different turbulence production and mixing mechanisms, and leads to improper reproduction of the near flow [1].

However, blade signatures and rotational momentum have shown to be overshadowed by ambient velocity fluctuations in the far wake [2]. Porous disc models can create similar far wake as rotating models, making AD an adequate and appropriate substitution both at low and high inflow turbulence, typically from  $x/D = 3-4$  [14] [1] [2] [9] [?] [?]. and thus the disks are acceptable when studying wake interactions at wind farm scale. Bossuyt et al 2016 concluded that the experimental setup of a model wind farm is able to capture the main trends in mean row power and unsteady loading, making it useful for layout optimization studies.

Studies have found that the drag coefficient is only weakly dependent on Reynolds number, so it remains roughly constant for a range of wind tunnel velocities. However, there is a dependence, meaning predictions of drag force with low levels of turbulence may differ from drag force experienced when operating in highly turbulent flow [4].

## 2.0.1 Experimentally

Lignarolo et al 2016 [10] provided an experimental analysis of the near-wake turbulent flow of a wind turbine and a porous disc. finding similarities and differences. They concluded that even in the absence of turbulence, the results show a good match in many variables such as thrust and energy coefficient, velocity, pressure and enthalpy. However, the turbulence intensity and turbulent mixing varied. The results suggested the possibility to extend the use of AD in numerical simulations until the very near wake, provided that turbulent mixing is correctly represented. The underlying question is how much the near wake differs given similarity of dimension, axial force and extracted energy. The stronger fluctuations in the WT wake are due to the presence of concentrated tip vortices. They found the turbulence intensity of WT to be 2-4 times larger than for the AD wake in the near wake. Physics governing the turbulent mixing in the two wakes are intrinsically different. even in the absence of inflow turbulence, the velocity fields in the wakes are very

---

well comparable. Again, extend the use of AD in numerical simulations until the very near wake.

[10] also compared earlier experiments, showing a consistent decreasing drag coefficient with increasing porosity.

Also the other Lignarolo: [9] conducted an experimental study focusing on the comparison between the wake of a turbine and an AD. WT wake characterized by complex dynamics of tip vortex development and breakdown, and turbulent fluctuations. Wake of AD is instead characterized by isotropic random fluctuations. Looking into the limitations.

It is known that AD misestimates the effects of flow turbulence, due to the absence of the blade flow and its tip-vortex development and breakdown (Barthelie 2007). The mixing process across the wake interface and ultimately the rate at which the wake recovers the flow momentum is incorrectly modelled.

The far wake region is typically less affected by the presence of the rotating blades.

Despite the popularity of the simplified numerical model, few experimental studies are available, which analyse the flow field in the wake of an AD [9]. Matching the diameter and thrust coefficient, the two give rise to the same wake expansion.

Blackmore et al [4] used experiments to investigate the effects of turbulence on the drag of solid discs and porous disc turbine simulators.

Aubrun et al (2013) [2] studied wind turbine wake properties, by comparing a non-rotating simplified WT, based on the AD concept, and a rotating model, to determine the limits of the simplified model to reproduce a realistic wake. Concluding that the wakes, in the modeled ABL, were indistinguishable after 3D downstream. (in relatively high turbulent inflow conditions. Discrepancies still exist at  $x/d = 3$  in low turbulent inflow conditions, but are relatively minor. So the simplified AD model seems to be usable to reproduce the far wake.

## **2.0.2 Use in CFD simulations**

Numerical simulations and experimental studies can complement each other for a better understanding.

As mentioned, wind turbines are large, on the order of hundreds of meters, with a typical spacing within a farm of 5-10 D, and a thickness of the blade on the order of 1m. In order to resolve the full turbine geometry, ideally one would need to build a mesh with submillimeter resolution in the blade BL inside a kilometer-scale computational box within the entire farm fits. As a consequence, we use a simplification: a model with an accuracy that generates the correct velocity deficit and TI in the far wake while ensuring that it is not too computationally demanding. Thus, most codes rely on AD. [11] [8] [7] Such models are an attractive alternative, as they require fewer grid cells and not as small grid dimensions, allowing larger time steps. This efficiency comes at the expense of resolving the fine details of the blade BL, but if the objective is the far wake, this trade off is reasonable and AD is more than acceptable. As with experiments, a porous disc with the same diameter that applies a similar thrust force upon the moving fluid as a set of rotating blades may

---

be used, but turbulence structures shed from the disk vary compared to the rotor in the near wake. Thus, AD is well suited for full wind farm computations. And work is being done in developing these models and comparing them to experimental results [7] [11], including a organized workshop to compare different state-of-the-art numerical models for the simulation of wind turbine wakes [8], especially comparing wakes produced from simulations to those produced with experiments.

Also on the computational area, more work related to AD is needed. For example, [11] claims the need for implementing a model for the wind turbine tower and nacelle to assess their impact on the turbine performance and wake profile.

Obtaining both real and experimental data is necessary in order to develop simulation methods and check simulated observations and predictions against actual wake characteristics. Experiments also provide data for computational model validation and for comparison for future work.

However, with such further development, a relatively inexpensive tool for assesment of flowfields and planning of wind farms would be at hand for the industry (to enable the industrial use of CFD), and the CFD AD could be an accurate and validated method for numerically modelling turbines [16] [7].

### **2.0.3 Developing the actuator disk**

One main issue remains, as there is no standard for designing and making the experimental actuator discs. Bossuyt et al (2016) [5] used a symmetric design, with a solidity that decreases with radial direction. Lignarolo et al (2016) [10] used a layered fine metal mesh, considered as a grid turbulence generator, while Aubrun et al [2] used fine metal meshes with varying porosity at the center of the disc and at the outer edge. Blackmore et al (2013) [4] used a hole pattern to maintain approximately uniform porosity across the radius. Aubrun et al [1] used both a metallic mesh with uniform porosity and a porous disc of plywood with radially non-uniform porosity. Sforza et al (1981) [16] used perforated metal plates, while Pierella and Sætran [15] used wooden grids. Myers et al (2010) [13] used PVC plastic for their discs. Even though the simulated turbine will vary, and thus the diameter, porosity and drag coefficient of the disc, a standard design creating the desired wake would be practical to create uniformity and comparability between experiments, and to save time so that every researcher around the world does not need to start the phase by developing their own disk.

Neunaber [14] cut her disk from an aluminium plate in a non-uniform matter. She also highlighted that she had a 100% blockage in the center, where the nacelle is located in the case of a turbine, and that blockage should vary linearly similar to a real turbine.

Another detail to take into consideration at this point is the wind-tunnel blockage effects created by the turbine models which may affect the wake. Thus, it is desired for the discs to be small [16].

Also wanted further work, as to explain why a smaller diameter porous disc resulted in lower drag coeff than the larger diameter disc with same porosity. [4]

---

Nevertheless, in a direct experimental comparison of turbulent flow in the near wake, a porous disk (with same dimension and axial force as a rotating turbine) is currently not available [10]. Main drivers are porosity, structural stiffness, wake-flow uniformity

# Chapter 3

## Method

In the following, the process of designing, creating and testing the actuator disks will be presented, as well as the experimental setup.

Ikke homogen freestream men wall effects definer spatial axes og origo

### 3.1 Experimental setup

In order to measure the drag on the wind turbine models and the actuator disks, a wind tunnel and a force plate is needed as part of the experimental setup. There was also the need to construct a rig on which the turbines could be placed inside the wind tunnel.

#### 3.1.1 Force measurer, wind tunnel and associated equipment

The wind tunnel used is one meter wide and a half meter tall. It has a maximum velocity of 35 m/s and a turbulence intensity of ... One can get inside the wind tunnel by removing a glass window which is ... m wide and ... m tall. The wind velocity can be changed by manually turning a wheel that changes the position of the valves in the tunnel. In the bottom plate of the tunnel there is a small hole, making it possible to connect the item one is measuring forces on to the load cell underneath the tunnel.

Underneath the wind tunnel is a force plate of the type AMTI BP400600HF 1000, able to measure the force and moments components along the x-, y- and z-axes. It can measure forces as low as ... and has an accuracy of ...

The voltage signal from the load cell is sent through an amplifier. Afterwards, it is sent through a low pass filter, with a cut-off frequency of 1000 Hz. The data was treated using LabView.

---

Inside the tunnel there is a sensor measuring the temperature, and a pitot tube measuring the pressure.

A potential uncertainty related to the wind tunnel is the fact that the pitot tube, which measures the pressure and is used to quantify the wind velocity, is placed in the centre of the tunnel. Thus, the velocity measured is not necessarily the same as the velocity that hits the actuator disks close to the ground of the tunnel. Due to wall boundary layers, the velocity hitting the disks is likely lower than the measured and registered velocity.

### **3.1.2 The rig**

The test rig consisted of a magnetic steel bar of 0.5 m stretching across the width of the wind tunnel, on top of a aluminium cylinder which connects the bar to an aluminium plate, that in turn can be strapped to the load cell underneath the wind tunnel. The bar was lifted about a centimeter above the ground floor of the tunnel. The measurements can be seen in the figure.

Initially, it was desired to have the steel bar be almost as long as the width of the wind tunnel, in order to avoid affecting the flow outside of what is already the boundary layer in the tunnel. Similarly, it was desired to have the hub of the turbines exactly in the vertical middle of the tunnel, to avoid the boundary layers. However, this was not doable, as the hole in the bottom of the wind tunnel was limited in size, which meant that the steel bar could only be connected to the load cell underneath the tunnel through one aluminium cylinder with a small diameter of about 2 cm. The length of the metal bar had to be shortened in order to avoid bending and flapping.

## **3.2 Wind turbine models**

The two-bladed rotating wind turbine models are the property of KTH in Stockholm. They have a diameter of 45 mm, and a hub height of approximately 65 mm. Magnets are incorporated into the bottom of the models.

## **3.3 The actuator disks**

Currently, there are no standard way of designing actuator disks. Some designs that have been tested are the circle shaped metal grid, and the spider web design, as here... Another possible method that has been to create two actuator disks that are connected and that can be rotated relative to each other, in order to change the solidity while the experiments are running. However, this seemed harder to achieve at such small scales as are relevant in this work.

### **3.3.1 Computer-aided design and 3D printing**

The actuator disks, as well as their stands, were designed using SolidWorks. Cura was used to turn the designs into readable code for the 3D printers, and the parts were then

---

printed using a printer of the type Ultimaker 2+. The material used was PLA.

A significant limitation occurred during the design process. The 3D printers available could not print thinner than 0.4 mm, meaning that each line in the disks had to be at least 0.4mm. However, printing lines of 0.4mm proved troublesome, and it was decided that all lines should be equal to or thicker than 0.5 mm. This is a significant number given that the disks are in themselves of such small dimensions. So it turned out that there will be a limit to how porous the disks can be made.

In general, a concern when using 3D printers is the fact that the print is not a hundred percent equal to the design - small variations may occur, making the actuator disks with the same design slightly different from each other. These slight variations matter more when the overall size of the design is so small compared to a larger design, however, the variations are still so few and small that they are considered to have close to no effect on the solidity or in making the disks differ from each other.

### **3.3.2 Design of the tower**

The tower was designed to have the exact same dimensions as the given wind turbine model's tower. Most importantly, it had a hub height of 65 mm. Underneath there was made a hole that could fit a cylindrical neodymium magnet with a diameter of 10 mm, a height of 2.5 mm and a strength of 0.9 kg. The actuator disks were made to be interchangeable, and the end of the tower where the actuator disks will be connected is made slightly thinner in order to fit into the designated holes in the actuator disks.

Three towers were printed.

### **3.3.3 Actuator disk design**

The actuator disks were designed with a diameter of 45 mm, to match the wind turbine models. The thickness of the disks is 2.5 mm.

Two different designs of actuator disks have been tested. The first has numerous equally-sized holes spread symmetrically around the centre point of the disk. This design is meant to be similar to those actuator disk designs made by a thin metal grid. The second design is also symmetric around the centre point, but this one has rectangular, however filled in to avoid sharp corners, holes that vary in size with radial distance, increasing in size as the radial coordinate increases.

For each of these configurations, two degrees of solidity was used as an initial try. The chosen values were 60% and 40%. A solid disk was also made and tested as a reference case.

Each disk was as mentioned made with a small hole in the centre that was used to connect the stand to the disks. Thus, this hole was filled in during the tests in the wind tunnel, and did not affect the solidity.

Three disks of each design and solidity were printed.

---

Based on the resulting drag profiles from the initial round of testing, two sets of actuator disks with a solidity of 35% were designed and made. The first was made based on the design with equally sized holes. Due to the mentioned limitations regarding the printing thickness, there was a limit to how low the solidity could get, and providing a solidity less than 39% proved problematic. Hence the design was slightly changed, allowing for the holes to also cover the edges of the actuator disk. It was kept in mind that this results in a different disk circumference, and that this might result in a drag force unrelated to the previously tested disks. The second was made as the designs with rectangular holes that vary in size with radial distance.

### 3.4 Testing

The rig was connected to the force plate using bolts, in such a way that the aluminium cylinder came up through the hole on the bottom of the tunnel. The rest of the hole was covered with thick tape. Careful consideration was taken when adding the tape, so that the aluminium cylinder did not touch anything, as that would affect the force measurements.

Given that the size of the wind turbine models is quite small, the turbines were tested in the wind tunnel three at a time, to ensure that the drag would be of an order that the instruments were able to measure and of an order where slight changes in the design resulting in slight changes in drag would be noticeable. The turbines were placed with a distance of 4D between them along the steel bar. The same was the case for the actuator disks.

Even though the turbine models were magnetic, it proved problematic to make them stay in the same position, with the turbine perpendicular to the wind direction, as the wind velocity increased. Thus, the models were connected to the steel bar using small pieces of tape. The 3D printed towers were able to stay in the right position on the base by themselves, still they were taped to the base like the rotating turbine models, to make sure the cases were comparable.

As the drag is the force of interest in this work, only the force in the x-direction is measured. The force was measured for five different wind velocities; 5 m/s, 7.5 m/s, 10 m/s, 12.5 m/s and 15 m/s. This corresponds to Reynolds numbers all of the order  $10^4$ . Since the velocity was changed by manually turning a wheel, a slight difference in the velocities occurred between the different measurements.

The force plate drifted over time, as is often the case with force measuring equipment. To take this into consideration when measuring the forces, zero measurements were conducted before and after every measurement. A 20 second tare measurement was first conducted. The wind tunnel was then turned on, with the velocity initially set to about 1 m/s, and then turned up to the wanted value. A measurement lasting one minute was then conducted. The velocity was once again reduced to about 1 m/s, and the wind tunnel was shut off. After the wind tunnel had quieted down and there was close to no moving air inside, another 20 second tare measurement was conducted. When measuring, a sampling rate of 1000 samples per second was used.

Besides measuring the drag on the rotating turbine models and on all the different sets of



---

actuator disks, a measurement was also conducted measuring only the drag on the base and the towers, without having any disks connected to them.

Define spacial axes!

## 3.5 Calculations

For each disk at each wind velocity, the data collected from the wind tunnel consisted of a time series of voltages corresponding to the measured force and the measured wind velocity, as well as the times for when the first zero measurement and the second zero measurement was conducted and when the 60 second measurement started. Using Matlab, this data was treated.

A linear drift of the force plate was assumed. Thus, using the two zero measurement values, a linear function approximating the drift was created. The part of this linear function corresponding to the 60 seconds where the force measurement was conducted, was extracted. For each measured force in the time series, the corresponding drift was subtracted. After, the average force over the time series was calculated, as well as the variance and standard deviation.

In the same matter, the drift was subtracted and the average force was calculated for the measurements of only the base and the tower. This was done for each of the different wind velocities. These averages were then subtracted from the averages calculated earlier, so that the final drag force was the force only on the disks, excluding the towers and the base.

Finally, this calculated drag was divided by three, so as to only consider the drag on one disk. This force was used in calculating the drag coefficient, as well as the total swiping area of the rotating turbine model, being  $\pi r^2$ .

Another value collected from the measurements was the average temperature during the 60 seconds of measuring, used to decide on the appropriate value for the air density when calculating the drag coefficient.

Removing the towers: [1] concluded that the discrepancy in rod fixation and distance between wall and disc center can generate different wake downwasg that might explain differences.

## Results & Discussion

After conducting the measurements, profiles showing the drag coefficient as a function of the wind velocity could be created for each set of disks.

### 4.1 Rotational WT model

The first measurement conducted using three rotating WT models resulted in a drag coefficient that was relatively independent of wind velocity for four of the measured wind velocities, but with a significant deviation at 5 m/s. To investigate whether this deviation was due to a measurement error, a second measurement was conducted, this time using three new rotating WT models. This second measurement gave more of an expected result at 5 m/s, however showed a deviation at 15 m/s. Thus, a third measurement, once again with three new rotating WT models, was conducted. Finally, a fourth measurement was carried out, this time using the same models as during the third measurement. The resulting drag coefficients can be seen as a function of wind velocity in figure 4.1.

As can be seen, there is some variation between the different measurement point. The values from the third and the fourth measurement are quite similar at 5 m/s, 7.5 m/s and 12 m/s, and at 15 m/s, they completely overlap. This may show that the measurement is repeatable, and that one of the reasons for the varying results is simply that the rotating WT models have small differences, for example related to the friction of the rotating blades and how well they are connected. Be it too tight, there will be added friction. Be it too loose, the blades may start to vibrate. However, even between the third and fourth measurement, there is a noticeable difference at 7.5 m/s, showing that differences between the WT models is not the only cause for the varying results.

Other possible causes of this variation may be related to noise and fluctuations in the applied wind velocity and in the force plate.

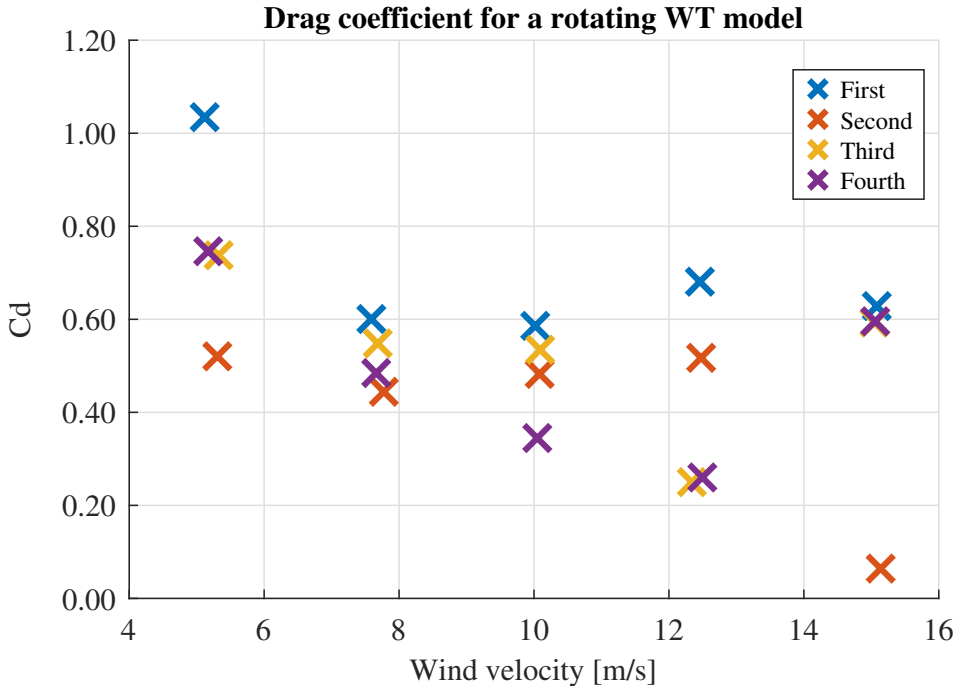


**Figure 4.1:** The drag coefficient for the rotating WT models, obtained through four rounds of measurements.

To investigate the results further, the drag resulting from the different measurements are pictured as a function of wind velocity in figure 4.2

As can be seen, the drag at 12.5 m/s is lower than the drag at 10 m/s for the third measurement, and the drag at 15 m/s is lower than the drag for 12.5 m/s for the second measurement. This is not physical, and thus it is assumed that these two values are errors. The drag measured during the fourth measurement coincides with the disregarded drag from the third measurement, and is thus also regarded as an outlier. The wind tunnel did, for some unknown reason, seem to produce larger amounts of noise on the signal for velocities between 11 and 13 m/s. The drag at 10 m/s for the fourth measurement is higher than the drag at 7.5 m/s, however the value is lower than for all the measurements which seem to coincide quite well, and thus this value is considered as an outlier. The initial suspicious value, measured at 5 m/s in the first measurement, results in a  $C_d$  larger than one, which seems unlikely, and hence this value is also regarded as an outlier.

The outlier seem to be spread out both in terms of velocity at which they occur and in terms of whether they exceed or fall below the other values. One can argue that if taking a large number of new measurements, they would have a Gaussian distribution about a mean, and that taking the average of the values that seemingly coincide would be representative for this total mean.

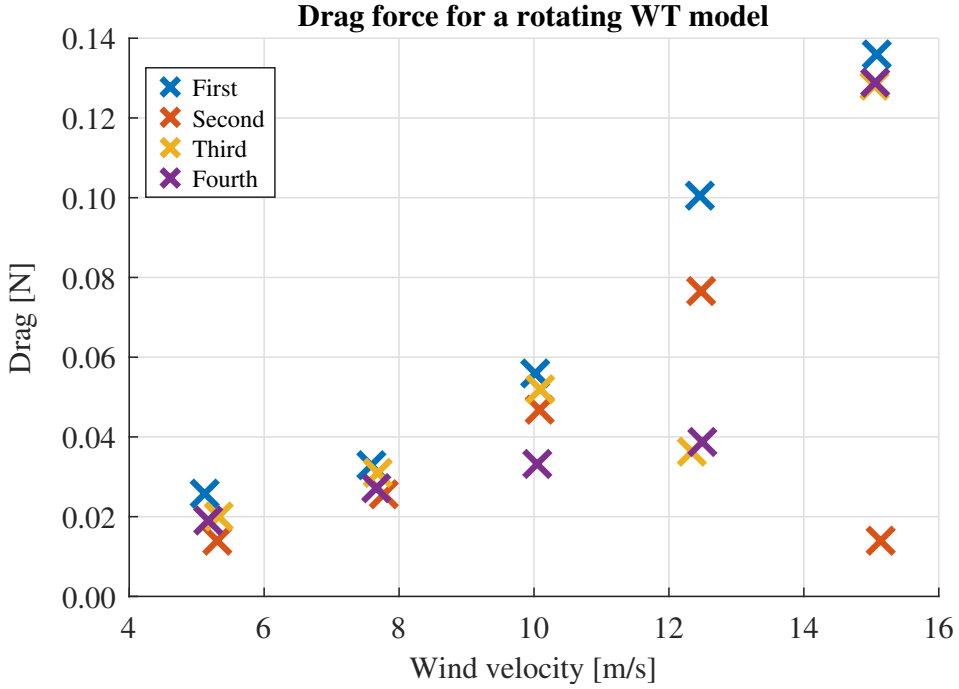


**Figure 4.2:** The measured drag for the rotating WT models, obtained through four rounds of measurements.

Thus, in order to achieve a representative value for the drag coefficient of the rotating WT models, the outliers were removed, and the average of the remaining drag coefficients was taken. This resulted in the drag coefficients seen in figure 4.7.

Assuming that  $C_d$  is Reynolds number independent for such a short span at Reynolds numbers, the average over these measurement points is taken, resulting in an average  $C_d$  of 0.585. Based on all the applied values, the standard deviation at hand is... Thus, when creating the ADs, this is the desired drag coefficient.

## 4.2 Drag on the ADs

The drag coefficient on the produced ADs has been studied. Initially, the solid disk, used as a reference case, produced the drag seen in figure ?? and the drag coefficient seen in figure ?. Further, the drag and the drag coefficient for the two types of disks with 60% solidity can be seen in figure ?? and ??, respectively. For both, the drag is seen to increase with increasing wind velocity, as one would expect.

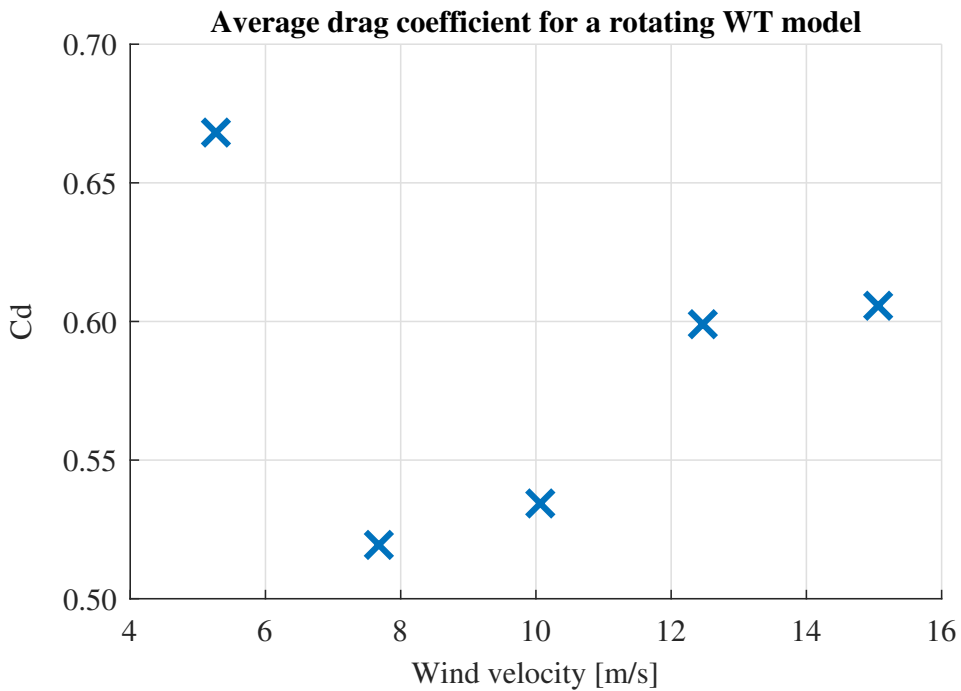


**Figure 4.3:** The average drag coefficient for the rotational WT models for each wind velocity, based on the four conducted measurements, after removing the assumed wrongful outliers.

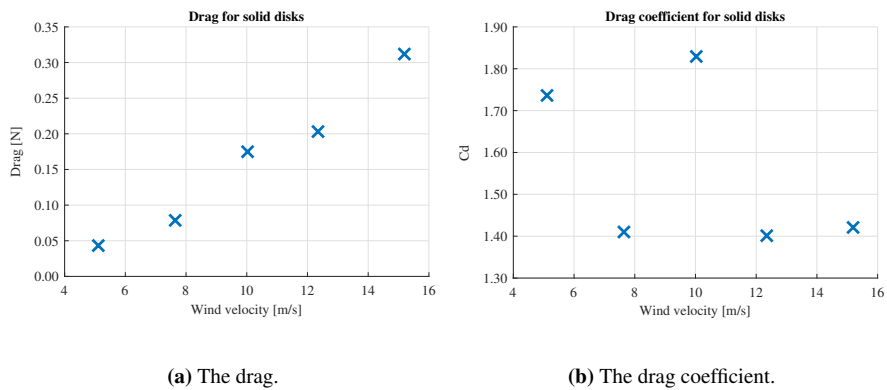


**Figure 4.4:** Using the solid disk.

## 4.3 Noise

## 4.4 Possible sources of error

Temperature changes

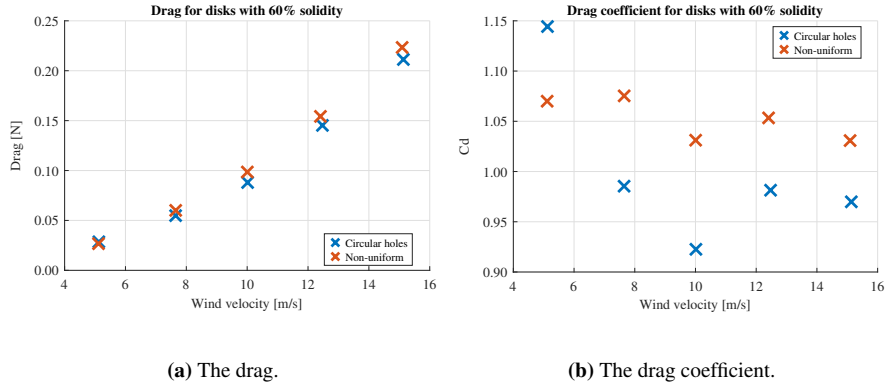


**Figure 4.5:** Using the disks with 60% solidity.

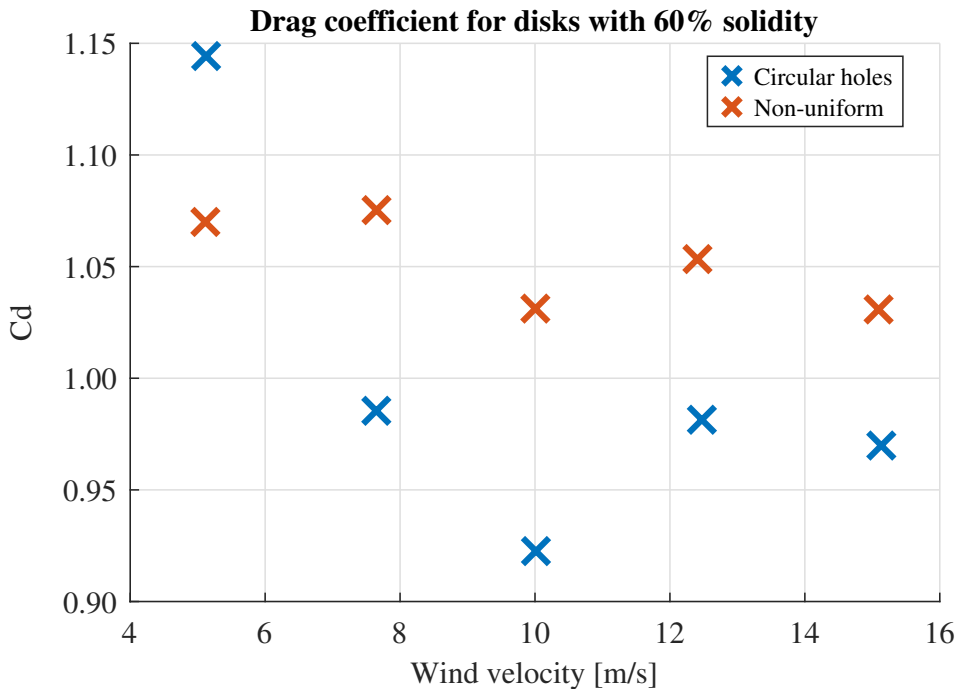


**Figure 4.6:** The drag coefficient for the disks with 60% solidity.

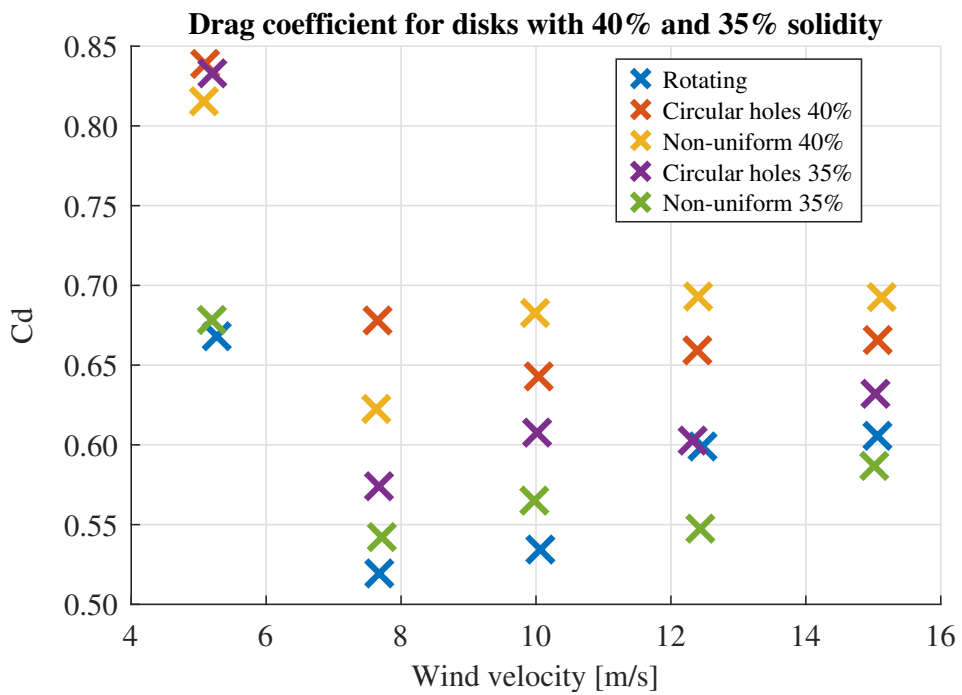


**Figure 4.7:** The drag coefficient for the disks with 40% and 35% solidity, compared to the average drag coefficient of the rotating disks.

# Chapter 5

## Future work

A natural extension to this work would be to create more actuator disks, with solidities in between 35% and 40%, to see if it is possible to match the drag coefficient profile of the rotating turbine models even better.

What I will do in my masters

Future plans and outlook Describe what you will do moving forward with this data for next term. Maybe even propose a matrix of tests you intend to look at or write a little bit about the problems in the area you intend to investigate and how you will solve them.



# Chapter 6

## Conclusion

WORKED REALLY WELL.

Conclusions Bring up the main points from the document, highlighting the method, results, conclusions, and where you will go next. This will be the last thing the grader reads, so you really want to remind the reader of all the good work you did.

wire mesh

bartheime og jensen, reduseres 20 prosent, derfor må vi finne ut om dette funker

google scholar kanskje oria for drag thrust delen

betz limit

35 sider vurderingskriterioer

# Bibliography

- [1] S. Aubrun, M. Bastankhah, R.B. Cal, B. Conan, R.J. Hearst, D. Hoek, M. Hölling, M. Huang, C Hur, B. Karlsen, I. Neunaber, M. Obligado, J. Peinke, M. Percin, L. Sae-tran, P Schito, B. Schliffke, D. Sims-Williams, O. Uzol, M.K. Vinnes, and A. Zasso. Round-robin tests of porous disc models. *Journal of Physics: Conference Series*, 1256:012004, jul 2019.
- [2] S. Aubrun, S. Loyer, P. Hancock, and P. Hayden. Wind turbine wake properties: Comparison between a non-rotating simplified wind turbine model and a rotating model. *Journal of Wind Engineering and Industrial Aerodynamics*, 120:1–8, 09 2013.
- [3] R. J. Barthelmie and L. E. Jensen. Evaluation of wind farm efficiency and wind turbine wakes at the nysted offshore wind farm. *Wind Energy*, 13, 04 2010.
- [4] Tom Blackmore, William Batten, Gerald Muller, and AbuBakr Bahaj. Influence of turbulence on the drag of solid discs and turbine simulators in a water current. *Experiments in Fluids*, 55, 12 2013.
- [5] Juliaan Bossuyt, Michael Howland, Charles Meneveau, and Johan Meyers. Measurement of unsteady loading and power output variability in a micro wind farm model in a wind tunnel. *Experiments in Fluids*, 58, 12 2016.
- [6] S. Cannon, F. Champagne, and A. Glezer. Observations of large-scale structures in wakes behind axisymmetric bodies. *Experiments in Fluids*, 14:447–450, 05 1993.
- [7] M.E. Harrison, William Batten, Luke Myers, and AbuBakr Bahaj. Comparison between cfd simulations and experiments for predicting the far wake of horizontal axis tidal turbines. *Renewable Power Generation, IET*, 4:613 – 627, 12 2010.
- [8] Lorenzo Lignarolo, Dhruv Mehta, Richard Stevens, Ali Yilmaz, Gijs Kuik, Søren Andersen, Charles Meneveau, Carlos Ferreira, Daniele Ragni, Johan Meyers, Gerard van Bussel, and Jessica Holierhoek. Validation of four les and a vortex model against stereo-piv measurements in the near wake of an actuator disc and a wind turbine. *Renewable Energy*, 94:510–523, 08 2016.

- 
- [9] Lorenzo Lignarolo, Daniele Ragni, Carlos Ferreira, and Gerard van Bussel. Kinetic energy entrainment in wind turbine and actuator disc wakes: An experimental analysis. *Journal of Physics: Conference Series*, 524:012163, 06 2014.
  - [10] Lorenzo Lignarolo, Daniele Ragni, Carlos Ferreira, and Gerard van Bussel. Experimental comparison of a wind-turbine and of an actuator-disc near wake. *Journal of Renewable and Sustainable Energy*, 8:023301, 03 2016.
  - [11] Luis Martínez Tossas, Matthew Churchfield, and Stefano Leonardi. Large eddy simulations of the flow past wind turbines: actuator line and disk modeling: Les of the flow past wind turbines: actuator line and disk modeling. *Wind Energy*, 18, 04 2014.
  - [12] Johan Meyers and Charles Meneveau. Optimal turbine spacing in fully developed wind farm boundary layers. *Wind Energy*, 15:305 – 317, 03 2012.
  - [13] Luke Myers and AbuBakr Bahaj. Experimental analysis of the flow field around horizontal axis tidal turbines by use of scale mesh disk rotor simulators. *Ocean Engineering*, 37:218–227, 02 2010.
  - [14] Ingrid Neunaber. *Stochastic investigation of the evolutoon of small-scale turbulence in the wake of a wind turbine exposed to diffeent inflow conditions*. PhD thesis, Carl von Ossietzky Universitat Oldenburg, 11 2018.
  - [15] Fabio Pierella and Lars Sætran. Effect of initial conditions on flow past grids of finite extension. *17th Australasian Fluid Mechanics Conference 2010*, 01 2010.
  - [16] P. Sforza, P. Sheerin, and M. Smorto. Three-dimensional wakes of simulated wind turbines. *Aiaa Journal - AIAA J*, 19:1101–1107, 09 1981.